

Density of States and Conductivity of Granular Metal or Array of Quantum Dots

Jingshan Zhang and Boris I. Shklovskii

Theoretical Physics Institute, University of Minnesota, 116 Church Street S.E., Minneapolis, Minnesota 55455
(February 8, 2020)

The conductivity of a granular metal or an array of quantum dots usually has the temperature dependence associated with variable range hopping within the soft Coulomb gap of density of states. This is difficult to explain because neutral dots have a hard charging gap at the Fermi level. We show that uncontrolled or intentional doping of the insulator around dots by donors leads to random charging of dots and finite bare density of states at the Fermi level. Then Coulomb interactions between electrons of distant dots results in the soft Coulomb gap. We show that in a sparse array of dots the bare density of states oscillates as a function of concentration of donors and causes periodic changes in the temperature dependence of conductivity. In a two-dimensional random array similar behavior can be achieved by charging of dots by a gate. In a dense array of dots the bare density of states is totally smeared if there are several donors per dot in the insulator.

I. INTRODUCTION

Conduction of samples where metallic granules are surrounded by some kind of insulator (granular metals) have been studied intensively for decades^{1–9}. If volume fraction of the metal x is large, metallic granules touch each other and conductivity is metallic. When x decreases and crosses percolation threshold x_c , granules become isolated from each other and granular metal goes through metal-insulator transition. It is generally observed^{1–3} that at the insulator side of transition the temperature dependence of conductivity obeys

$$\sigma = \sigma_0 \exp \left[- \left(\frac{T_0}{T} \right)^{1/2} \right]. \quad (1)$$

Recently, similar temperature dependence was observed in doped systems of self-assembled germanium quantum dots on the silicon surface¹⁰ and CdSe nanocrystal thin films¹¹. Below we talk about both granular metal and semiconductor dot structures universally using the word dot for brevity.

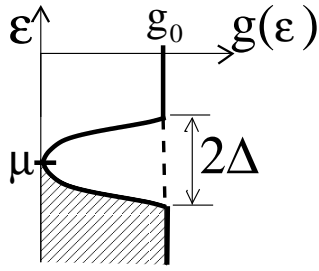


FIG. 1. The shape of Coulomb gap in the vicinity of the Fermi level. Bare density of states in the absence of long range Coulomb interaction is shown by the dashed line. Occupied states are shaded.

In doped semiconductors the temperature dependence of Eq. (1) is also widely observed at low temperatures⁴. It is interpreted as the variable range hopping conductivity between impurities in the presence of the Coulomb

gap^{4,12} of the density of states (DOS) and is called the Efros-Shklovskii (ES) law. In a n -type lightly doped compensated semiconductor all acceptors are negatively charged and randomly situated, an equal number of donors are charged positively. Together all random charges create a random potential shifting donor level up and down. This results in finite bare DOS $g_0(\mu)$ at the Fermi level μ . Long range Coulomb interaction of localized electrons then produces the parabolic Coulomb gap in DOS

$$g(\varepsilon) = \frac{3}{\pi} \kappa^3 \varepsilon^2 / e^6 \quad (2)$$

at the Fermi level (Fig. 1) leading to ES law with $T_0 = C \cdot e^2 / \kappa \xi$, where C is a constant factor, κ is dielectric constant and ξ is the localization length.

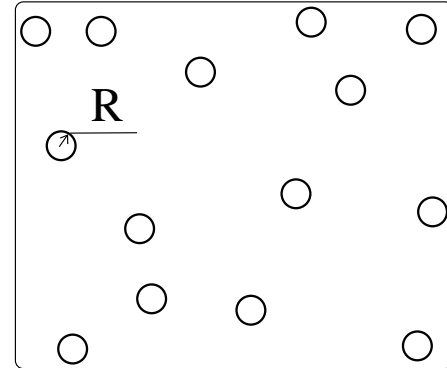


FIG. 2. A sparse array of same size neutral metallic dots surrounded by an insulator.

In contrary to a doped semiconductor, in an array of neutral dots the bare DOS at the Fermi level $g_0(\mu) = 0$ and there is no justification for ES law, which requires a nonzero $g_0(\mu)$ to begin with. Let us consider a sparse array of dots with the same radius R shown on Fig. 2. Charging energy levels of such array are shown in Fig. 3. Here we assume that dots are large enough, so that spacing between charging levels $e^2 / \kappa R$ is much greater than

spacing between quantum levels of the dot with a given charge. Empty peaks in Fig. 3 correspond to energies necessary to charge a neutral dot by the first, second and so on electrons transferring them from the macroscopic piece of the same metal. Shaded (filled) peaks correspond to, taken with the sign minus, energies necessary to extract first, second and so on electrons from the dot, or in other words, this is density of states of holes. The Fermi level of the array is at zero between two peaks and coincides with the Fermi level of macroscopic piece of the same metal.

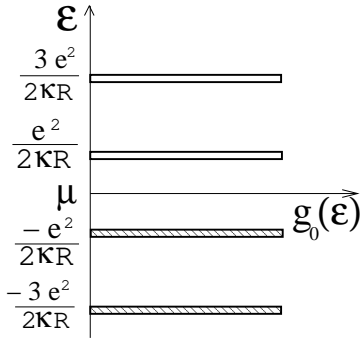


FIG. 3. The bare density of ground states (BDOGS) of a clean system of identical dots consists of equidistant peaks. Occupied states are shaded.

We want to emphasize that in each dot we are dealing with the ground state at a given number of electrons and exclude excited states (higher quantum levels) because the ground states of dots determine the low temperature hopping transport. Indeed, in the Miller-Abrahams network¹³ of resistances connecting all dots, the exponentially large activation factor of each resistance depends on probabilities of occupation of a dot by a given number of electrons. Exponential temperature dependencies of these probabilities, as well as the partition functions of dots are determined by ground state energies¹⁴. Thus, the density of states of the array we need can be called bare density of ground states (BDOGS).

Note that in a lightly doped semiconductor with several equivalent conduction band minima each donor has excited states close to the ground state, i. e. situation is similar to large dots. Still exponential temperature dependence of hopping conductivity depends only on BDOGS^{4,13}.

Let us illustrate the role of BDOGS in a clean sparse array (Fig. 3). In this case, conductivity requires activation of electron-hole pairs or in other words, transfer of an electron between two originally neutral dots. Obviously concentrations of positive and negative dots and the hopping conductivity obeys

$$\sigma = \sigma_0 \exp[-E_c/2k_B T] \quad (3)$$

independently of excited states, (Same result can be obtained in Miller-Abrahams resistor network approach.) where $E_c = e^2/\kappa R$ is the charging energy.

How then can we explain observation of ES law? Apparently BDOGS shown in Fig. 3 should be smeared in the vicinity of the Fermi level due to some kind of disorder.

A simplest source of disorder is distribution of sizes or capacitances of dots. Indeed, charging energies of larger dots are smaller and this can result in the low energy tail of the first empty peak of BDOGS and symmetric high energy tail of the first occupied peak. Still in a neutral system these tails do not overlap and $g_0(\mu)$ is zero, so that this kind of disorder does not lead to ES law. Sheng et al.¹ assumed that in a reasonably dense system of neutral granules there is a special distribution of distances between granules or their mutual capacitances, which can lead to ES law. This assumption was found incompatible with other experiments⁵. But more importantly it was noticed⁶ that in a system of large granules made of the same metal all granules remain neutral in ground state at any distribution of mutual and individual capacitances. Therefore, inter-granular excitation of electron-hole pairs has a gap.

This leads to an important conclusion that granular metal may have finite BDOGS $g_0(\mu)$ and show ES conductivity only if in the ground state of the system granules are charged⁴⁻⁹. Formally one can imagine that this happens if granules have different work functions^{4,6}. Several possible mechanisms of such fluctuations were discussed in literature. Chui⁷ suggested that very small dots can charge big dots in the case when the former are so small that their quantum level spacing exceeds the charging energy. We concentrate on the system of large enough dots and, therefore, ignore this possibility. Cuevas et al.⁸ claimed that even in large dots there are large fluctuations of the Fermi level δE_F due to random positions of neutral impurities in different dots. To our mind, this possibility can be rejected using for δE_F a simple estimate of typical fluctuation of the average potential in the metallic dot due to fluctuation of number of impurities there. For three dimensional case one easily gets $\delta E_F \sim E_F c^{1/2}/(k_F R)^{3/2}$, where c is relative concentration of impurities in the dot, k_F is Fermi wave-vector, and we assume that size of an impurity is of the order of k_F^{-1} and its potential $U \sim E_F$. At large R this energy is apparently smaller than charging energy $e^2/\kappa R$ even at $c \sim 1$, so that dots remain neutral. Baskin and Entin⁹ considered fluctuations of surface part of the dot energy as a reason of ionization of dots. Again if we assume that these fluctuations are result of random distribution of point-like impurities located on the dot surface we come to conclusion that corresponding fluctuation of energy decreases like $1/R^2$ and can not compete with the charging energy. Thus, simplest internal mechanisms of fluctuations of the work function mentioned above are too weak to charge array of three-dimensional dots.

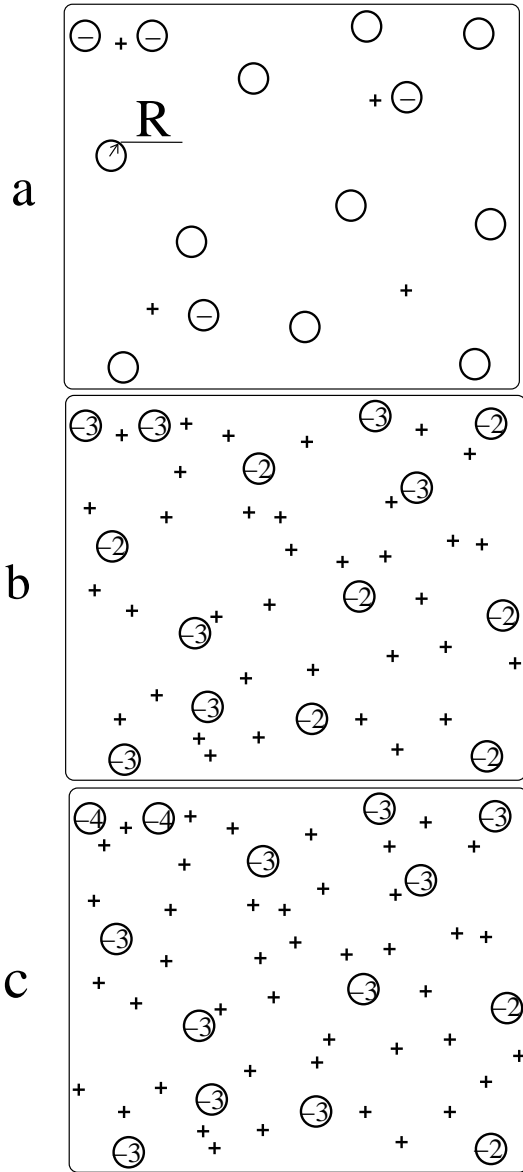


FIG. 4. A sparse array of dots with different concentrations of donors (+) in the surrounding insulator. a) $\nu = N_D/N \ll 1$, b) $\nu = 2.5$, c) $\nu = 3$.

In this paper we study a model of array of dots affected by external disorder, where the origin of charging and BDOGS g_0 is transparent and in some cases controllable. We assume that the insulator separating clean dots has a concentration of donors N_D with electron energy E_D higher than Fermi energy μ in dots, so that at low temperatures all donor donate an electron to dots and charge them. For a given concentration of dots N (Fig. 4) we can introduce the average number of extra electrons per dot $\nu \equiv N_D/N$, which by analogy with quantum Hall effect we can call the filling factor. Maximum number of electrons which can be added to a dot is $n_{max} \simeq (E_D - \mu)/(e^2/\kappa R)$. We assume that $\nu < n_{max}$ so that all donors lose their electrons. In the semiconductor language we are dealing with compensated p -type

semiconductor where dots play the role of multi-charged acceptors.

We start from sparse arrays of dots of the same radius R , which are randomly situated in space with concentration $N \ll (4\pi R^3/3)^{-1}$. We assume that the dots are big enough so that Coulomb effect over-weights quantum level spacing.

Then in Sec. V we consider several dense arrays of dots, one example of which is shown in Fig. 5. Clean metallic cubes are separated by thin layers of an insulator doped by donors. It is assumed that the tunneling conductance between two cubes $G \ll e^2/h$. We show that several donors per one dot can smear BDOGS.

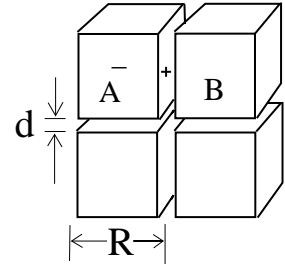


FIG. 5. A ‘super-dense’ array of dots. Only one donor is shown by + and electron donated by it is shown by -.

In the next section we summarize our main results for BDOGS at the Fermi level $g_0(\mu)$ as function of the filling factor ν , while the derivations are in Secs. III, IV and V.

II. SUMMARY OF RESULTS

Starting from sparse three dimensional arrays of dots, we see in Fig. 4 that doping introduces two types of charges: positive, empty donors and negatively charged dots. Both are randomly situated and create random potentials growing with ν . These charges result in two effects (Fig. 6). Firstly, the δ -shaped peaks in BDOGS $g_0(\varepsilon)$ become somewhat smeared, since the energy it takes to bring an electron to a dot is affected by the random potential (the effect is similar to that of gedanken random gate potential). As a result, each peak gets tails. Secondly, electrons coming from donors fill some dot states and hence move the position of the Fermi level up.

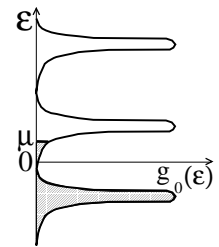


FIG. 6. BDOGS $g_0(\varepsilon)$ at a certain filling factor. Occupied states are shaded.

As a result $g_0(\mu)$ may oscillate with ν . For example, at $\nu = 1/2$ the Fermi level μ is in the middle of the BDOGS peak and for that reason $g_0(\mu)$ can be rather large. On the other hand, at $\nu = 1$ the Fermi level μ is in a tail between two BDOGS peaks, and $g_0(\mu)$ tends to be much lower. Actually the total dependence of $g_0(\mu)$ on ν is somewhat more complicated and consists of three parts, the growing part, the oscillating part and the saturation part (Fig. 7). The first (growing) part takes place at small ν (Fig. 4a), where the situation is similar to p -type semiconductors at low degree of compensation¹⁵. We get BDOGS growing linearly with ν

$$g_0(\mu) \sim \kappa \nu N^{2/3} / e^2 \quad (\nu \ll 1). \quad (4)$$

In the second (oscillating) part, μ typically dwells in BDOGS peaks, (1)

$$g_{max}(\mu) \sim \frac{N^{2/3} \kappa}{e^2 \nu^{4/3}} \quad (1 < \nu < \nu_s). \quad (5)$$

When ν is very close to integers, the Fermi level drop into minima of $g_0(\varepsilon)$ where

$$g_{min}(\mu) \sim \frac{\nu^{8/3} N^{5/3} R^2}{e^2 / (\kappa R)} \quad (1 < \nu < \nu_s). \quad (6)$$

Here $\nu_s \sim 1/(NR^3)^{1/4} \gg 1$ is the filling factor at which oscillations become relatively small and the third (saturation) part starts over. This happens because fluctuations of the Coulomb potential are so big that BDOGS is almost uniform everywhere

$$g_s \sim \frac{N}{e^2 / (\kappa R)} \quad (\nu > \nu_s). \quad (7)$$

The number of large oscillations ν_s is big only when dots are far from each other. Here and below we often omit numerical coefficients.

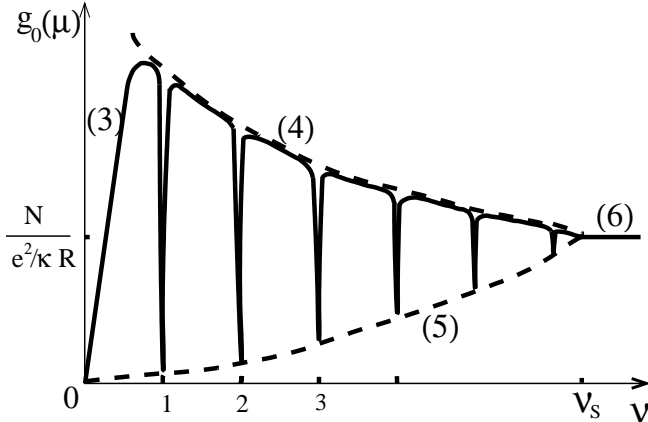


FIG. 7. BDOGS at the Fermi level $g_0(\mu)$ of a sparse array as a function of filling factor (solid line). The reference to the equation appropriate for a part of the curve is shown next to it. Dashed lines describe locations of minima and maxima of the oscillating part.

For less ideal arrays where the dots have slightly different sizes, the distribution of sizes can wash away the oscillations to a certain extent, making the line of maxima lower and the line of minima higher. As a result the two lines approach each other faster (ν_s is smaller) than the situation of identical sizes.

Oscillations of $g_0(\mu)$ lead to periodic transitions between the ES law and the Mott's law at a given low temperature as shown in Fig. 8. This happens because in the very vicinity of μ the long range Coulomb interaction creates the parabolic Coulomb gap (not shown in Fig. 6). The width of Coulomb gap as follows from Eq. (2) and Fig. 1 depends on g_0

$$\Delta \sim \sqrt{g_0(\mu) e^6 / \kappa^3}. \quad (8)$$

At large g_0 the Coulomb gap is wide ($\Delta \gg k_B T$) and the conductivity obeys the ES law (Eq. (1)), which does not depend on g_0 . At a very small g_0 the width of the Coulomb gap is smaller than $k_B T$ and becomes irrelevant for conductivity. In this case we arrive at the Mott's law region

$$\sigma = \sigma_0 \cdot \exp \left[- \left(\frac{\beta}{g_0(\mu) a^3 T} \right)^{1/4} \right], \quad (9)$$

with strong dependence on $g_0(\mu)$. Here β is a numerical coefficient⁴.

Oscillations of BDOGS $g_0(\mu)$ with ν lead to oscillations of other measurable quantities. It was shown¹⁶ that in systems with the Coulomb gap BDOGS $g_0(\mu)$ plays the role of the thermodynamic density of states $dn/d\mu$, where n is concentration of electrons, so that it determines screening radius of the system $r_s = (4\pi g_0 e^2 / \kappa)^{-1/2}$ used below for self-consistent calculations of BDOGS. One can also measure BDOGS at the Fermi level with help of extremely low temperature (lower than typical quantum level spacing) specific heat and microwave absorption^{4,17}

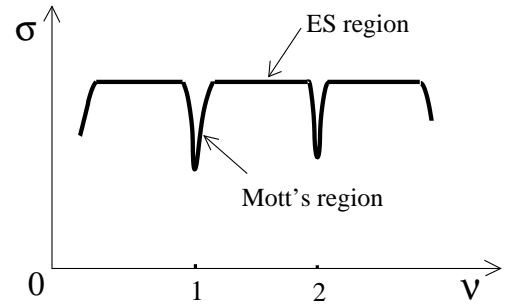


FIG. 8. Ranges of ES and Mott's laws alternating with growth of filling factor ν at a given low temperature.

Until now we talked about 3D arrays of dots. In Sec. IV we consider arrays of dots located in a 2D plane. In a 2D array dots can be charged by donors located in parallel to the plane (δ -layer)^{10,18}. In 2D case, however, there is a more practical way to charge dots using a plane metallic gate parallel to the plane of dots. At $\nu \gg 1$ results for $g_0(\mu)$ are almost independent on the way of charging, because most of the random potential is mainly created by dot charges. Dependence of $g_0(\mu)$ on ν in 2D qualitatively looks similar to the 3D case discussed above, but quantitatively it is somewhat different (see Sec. IV).

Dependence of $g_0(\mu)$ on ν in 2D should leads to oscillations of conductivity. Some oscillation were observed in Ref^{10,18}. But there are additional ways to measure this dependence in a gated in 2D structure. First¹⁰, one can study change of conductivity where the gate voltage charges dots. Second¹⁹, one can study inverse small signal AC capacitance of unit area $1/C$, which is related to the two-dimensional screening radius of the dot system $r_s = \kappa/(2\pi g_0 e^2)$ by equation

$$1/C = 4\pi\kappa(d_0 + r_s), \quad (10)$$

where d_0 is distance from gate to the plane of dots. This method is similar to magneto-capacitance measurements in quantum Hall effect²⁰.

Until now we talked about sparse arrays of dots. For a sparse array of dots the variable range hopping conductivity is measurable only when the tunneling length in insulator is large enough. This probably can be achieved in some cases in narrow gap semiconductors. Otherwise conductivity is so small that it can not be measured. In this case, thermodynamic measurements of oscillating quantities may be more convenient.

It is much easier to measure conductivity in a dense array of dots. Actually most of cited experiments are done at $NR^3 \sim 1$ or $d \ll R$. In Sec. V we study “super-dense” limit $d \ll R$ (Fig. 5) and show that in the dense array BDOGS as a function of the average number of donors per dot ν behaves as shown in Fig. 9. At $\nu \ll 1$ BDOGS is very small and grows super-linearly with ν (like ν^3), and at $\nu \sim 1$ it saturates at the value $\tilde{g}_s \sim \kappa/(e^2 R D d)$.

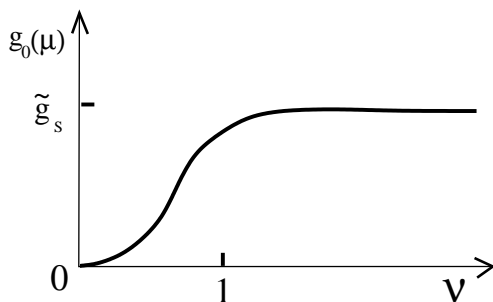


FIG. 9. BDOGS at the Fermi level $g_0(\mu)$ of a “super-dense” array as a function of filling factor ν .

III. BDOGS IN SPARSE THREE-DIMENSIONAL ARRAYS.

1. Saturation of BDOGS

With enough impurities the BDOGS is strongly smeared and it approaches an averaged value given by Eq. (7). This happens when the fluctuation of potential γ is large enough, namely

$$\gamma > e^2/\kappa R. \quad (11)$$

In order to find the critical ν_s of the saturation BDOGS, let us study the fluctuation of electric potential. For a given quantum dot, all the charges within a distance of the screening radius r_s contribute into a collective Coulomb potential. There are two kinds of charges, positive donors and negative dots. Let us compare the charge fluctuations made by them. The average number of impurities within r_s is $N\nu r_s^3$, with a typical charge fluctuation $e\sqrt{N\nu r_s^3}$. For the charged dots, the typical fluctuation of dot number in r_s is $\sqrt{Nr_s^3}$, and each dot carries a charge of $e\nu$ on average, so the typical charge fluctuation is $\nu e\sqrt{Nr_s^3}$. At $\nu \gg 1$ the charge fluctuations produced by charged dots are larger than that of donors, so that the fluctuation of the potential energy of an electron is mostly related to charge fluctuations of dots

$$\gamma \sim \frac{\nu e^2}{\kappa r_s} \sqrt{Nr_s^3}. \quad (12)$$

On the other hand, the BDOGS at the Fermi level $g_0(\mu)$ determines the linear screening radius due to re-distribution of electrons between dots

$$r_s = \frac{1}{\sqrt{4\pi g(\mu)e^2/\kappa}} \sim \frac{1}{\sqrt{NR}}. \quad (13)$$

With the help of Eqs. (12) and (13), the requirement (11) becomes

$$\gamma \sim e^2 \nu (N/R)^{1/4} / \kappa > e^2 / \kappa R. \quad (14)$$

Therefore only at $\nu > \nu_s \equiv 1/(NR^3)^{1/4}$ can we have big enough potential fluctuation. At $\nu > \nu_s$ BDOGS is smeared so strongly that at a given ν BDOGS $g(\varepsilon) \sim g_s$ at all energies, and $g_0(\mu)$ does not depend on the position of μ any longer.

2. Line of maxima of oscillating BDOGS.

When ν is close to a half-integer $M - 1/2$ (M is an integer) the Fermi level is in the middle of the M th peak in the BDOGS of dots (Fig. 10). Distribution of charges on dots in this case is illustrated by Fig. 4b.

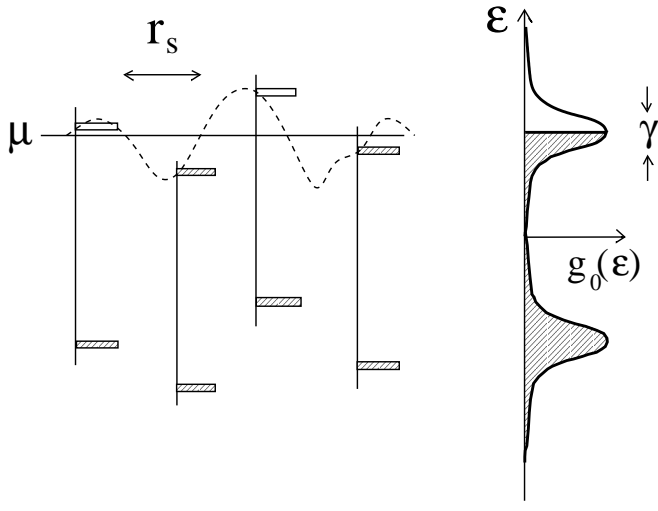


FIG. 10. The origin of g_{max} . The solid horizontal line is the Fermi level, the dashed line is the fluctuating potential energy. Two peaks of BDOGS of the array are shown, as well as two corresponding levels of 4 dots.

The single dot charging levels vary with the electric potential energy. The typical fluctuation of the potential energy is determined by Eqs. (12), which broadens the BDOGS peak (Fig. 10). The BDOGS at the peak is

$$g_{max}(\mu) \sim g_{peak}(\varepsilon) \sim \frac{N}{\gamma} . \quad (15)$$

In such a situation the linear screening radius is

$$r_s = \frac{1}{\sqrt{4\pi g_{max}(\mu) e^2 / \kappa}} . \quad (16)$$

At $1 < \nu < \nu_s$ Eqs. (12), (15) and (16) self-consistently determine all three unknowns: the BDOGS $g_{max}(\mu)$, the screening radius and the typical fluctuation of the potential energy. We arrive at Eq. (5) and

$$r_s \sim \nu^{2/3} / N^{1/3} \gg N^{-1/3} , \quad (17)$$

$$\gamma \sim e^2 \nu^{4/3} N^{1/3} / \kappa . \quad (18)$$

It is clear from Eq. (5) that g_{max} arrives at the value $g_s \sim N / (e^2 / \kappa R)$ when $\nu \sim \nu_s \equiv 1 / (N R^3)^{1/4} \gg 1$. Note that the theory of this subsection is similar to Ref.²¹.

3. Line of minima of oscillating BDOGS.

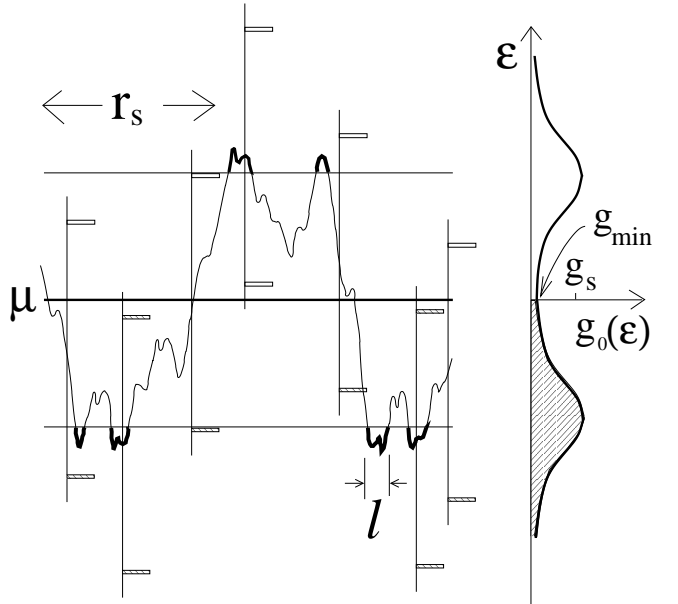


FIG. 11. The origin of g_{min} . The meandering line represents the fluctuating potential energy as a function of coordinate. The regions of the shortest size $\sim l$ where dots are completely filled with electrons or holes are shown with thicker lines. The solid horizontal line in the middle is the Fermi level, the other two horizontal lines correspond to the nearest peaks of an isolated dot. Two peaks of BDOGS of the array are shown, as well as two corresponding levels of 7 dots.

When ν is close to an integer M the Fermi level lies in the tail between the M th and $(M+1)$ th peaks in the BDOGS of dots. Due to the low BDOGS at tails, screening of the long-range fluctuations is weak and strongly nonlinear. The random potential fluctuation grows until it reaches $e^2 / 2\kappa R$, where levels of some dots cross the Fermi level (Fig. 11) and lose or gain an electron (see Fig. 4c). This picture is similar to the model of compensated semiconductor and we treat it below following ideas of Chapter 13 of Ref.⁴. Let us define r_s as nonlinear screening radius. As shown in Fig. 12 all space can be divided into blocks of size r_s with fluctuating excess charges $q \sim \nu e \sqrt{N r_s^3}$ which create potential $\gamma(r_s) \sim \frac{\nu e^2}{\kappa r_s} \sqrt{N r_s^3}$. This requires

$$e^2 / \kappa R \sim \gamma(r_s) \sim \frac{\nu e^2}{\kappa r_s} \sqrt{N r_s^3} \quad (19)$$

and we arrive at

$$r_s \sim \frac{1}{N \nu^2 R^2} . \quad (20)$$

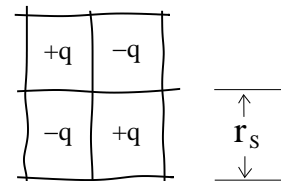


FIG. 12. Accumulation of dot charges due to fluctuation of number of dots within regions of size r_s .

The potential fluctuation forms wells and humps (Fig. 11). Electrons fall into wells and holes fall into humps. We will discuss the wells and electrons, although our discussion is equally applicable to humps and holes. Inside a well of size r_s there are other humps and wells of shorter range. Electrons inside wells find themselves in wells of smaller scale and so on until they reach the shortest scale l .

The shortest range l can be determined by the fact that each dot accepts only one electron. The excess number of charges inside such a well is of the order $\nu\sqrt{Nl^3}$. The maximum number of electrons in the well is of the same order, otherwise the well turns into a hump. On the other hand the maximum number of electrons is Nl^3 so that $Nl^3 \sim \nu\sqrt{Nl^3}$. This gives

$$l \sim (\nu^2/N)^{1/3} \quad (21)$$

for the characteristic size of the shortest scale well, and

$$\gamma(l) \sim \frac{\nu e^2}{\kappa l} \sqrt{Nl^3} \sim \nu^{4/3} N^{1/3} e^2 / \kappa. \quad (22)$$

for the characteristic depth. It can be checked that $l \ll r_s$ as long as $\nu \ll \nu_s$, in accordance with our assumption.

As we said, in a cube of size r_s , the fluctuation of extra charge is $q \sim \nu e \sqrt{Nr_s^3}$ (Fig. 12), which is balanced by the screening charge $\Delta N r_s^3 e$ (ΔN is concentration of dots participating in screening):

$$\Delta N r_s^3 e \sim \nu e \sqrt{Nr_s^3}, \quad (23)$$

therefore

$$\Delta N \sim \nu^4 N^2 R^3. \quad (24)$$

With the help of Eqs. (22) and (24), one can estimate the BDOGS at the Fermi level as $g_{min}(\mu) \sim \Delta N / \gamma(l)$, and arrive at Eq. (6). For peaks of $g(\varepsilon)$ at $\varepsilon = \pm e^2 / 2\kappa R$ we have $g(\varepsilon) \approx g_s \gg g_{min}(\mu)$ (see Fig. 11).

At $\nu \sim \nu_s$ the shortest scale of wells and humps l approaches the longest scale of wells and humps r_s , and each dot can accept more than one electrons or holes because $\gamma > e^2 / \kappa R$. Therefore the non-linear screening crosses over to linear screening at $\nu \sim \nu_s$. At the same time the fluctuation of potential energy γ is big enough to smear the BDOGS. It can be checked that g_{min} and g_{max} merge to g_s at $\nu = \nu_s$.

4. Growing part of BDOGS.

When concentration of impurities is rather low, $\nu \ll 1$, an electron released by a donor would like to stay on a dot close to the donor. The common situation is a donor accompanied by one charged dot (1-complex), while some donors stay alone (0-complex), and some donors are accompanied by two charged dots (2-complex). Charge

conservation requires $N_0 = N_2$, where N_0 and N_2 are concentrations of 0- and 2-complexes. Two 1-complexes, one 0-complex (down-right corner) and one 2-complex (up-left corner) are shown in Fig. 4a.

At $\nu \ll 1$ nearly all donors are independent, and N_0 , N_1 and N_2 are proportional to ν . Therefore the Fermi level remains a constant and the BDOGS grows linearly with ν at $\nu \ll 1$.

The details of this problem is the same as in a weakly compensated doped semiconductors. It has been studied quantitatively¹⁵, counting the numbers of 0- and 2-complexes. The quantitative results are

$$N_0 = N\nu \exp\left(-\frac{4\pi}{3} \frac{e^2 N}{\kappa|\mu|^3}\right), \quad (25)$$

$$N_2 = 7.14 \cdot 10^{-4} \cdot \left(\frac{4\pi}{3}\right)^2 \cdot N\nu \left(\frac{e^2 N^{1/3}}{\kappa\mu}\right)^6, \quad (26)$$

$$\mu = -0.99 e^2 N^{1/3} / \kappa. \quad (27)$$

As the concentration of impurities $N\nu = N_0 + N_1 + N_2$ is not changed, the concentration of electrons on dots is controlled by the Fermi level μ , therefore

$$g_<(\mu) = \frac{dN_2}{d\mu} - \frac{dN_0}{d\mu} = 0.2\kappa\nu N^{2/3} / e^2. \quad (28)$$

We kept all coefficients in this subsection because they are known.

Thus $g_<(\mu)$ is proportional to ν and follows Eq. (4). This picture works well at $\nu \ll 1$. At $\nu \geq 1$ each dot is typically affected by more than one impurities. It is straightforward to check that Eq. (4) matches Eq. (5) at $\nu \sim 1$.

5. Periodic array of dots.

Above we have discussed sparse arrays in which the dots are situated randomly. Now we turn to a question, what if the dots are arranged periodically in space (Fig. 13)?

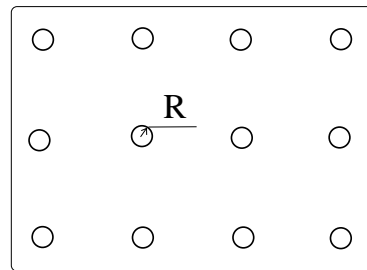


FIG. 13. A sparse periodic array of dots.

The qualitative picture in Fig. 7 is still mostly correct. At $\nu \gg 1$ there are still the oscillations of $g_0(\mu)$ with ν . One should notice that the strongly charged periodic dots do not contribute to the fluctuations of electric potential and only donors produce the fluctuations. As we discussed above these fluctuations are weaker than in the random sparse array. Therefore more donors are needed to smear BDOGS to the same extent. In other words, the lines of maxima and minima in this case converge slower and the value of ν_s is larger.

The linear growth of BDOGS at $\nu \ll 1$ shown in Fig. 7 is not valid in a periodic array, since 0- and 2-complexes originate from the random distribution of dots in space. In periodic array a typical donor donates an electron to the nearest dots and forms an electric dipole. It takes additional energy to take an electron out of a dipole and put it near another dipole. Therefore a hard gap is formed at the vicinity of the Fermi level. Only the rare cases where several donors are close to each other can produce non-zero BDOGS at the Fermi level. As a result $g_0(\mu)$ does not grow linearly with ν , but with higher power. The similar situation will be studied more thoroughly in the dense array of Sec. V. Therefore, here we gave only a brief description of the result.

IV. BDOGS IN A SPARSE TWO-DIMENSIONAL ARRAY

The $g_0(\mu)$ as a function of ν in 2D looks similar to 3D (Fig. 7). It also has growing part, oscillating part and saturation part. However, in 2D oscillations survive longer than in 3D, because the collective potential in 2D is much weaker. Indeed, the fluctuation of potential energy in 3D grows with r_s as a power law

$$\gamma_{3D} \sim \frac{\nu e^2}{\kappa r_s} \sqrt{Nr_s^3} \propto r_s^{1/2}, \quad (29)$$

while in 2D the long-range fluctuation of potential energy grows slower than logarithmically with r_s

$$\gamma_{2D} \sim \left(\int_{1/\sqrt{N}}^{r_s} \left(\frac{\nu e^2}{\kappa r} \right)^2 N r dr \right)^{1/2} \propto \sqrt{\ln(\sqrt{Nr_s})}. \quad (30)$$

Therefore the line of minima of oscillating part in 2D is quite different from that of 3D. The tail in the $g(\varepsilon)$ vs. ε curve is produced here by Coulomb interaction of nearest neighbor dots, and the minimum value of g appears to be (at $1 \ll \nu < \nu_s = 1/\sqrt{NR^2}$)

$$g_{min} \sim N^2 (\nu e^2 / \kappa)^2 / \varepsilon |_{\varepsilon \sim e^2 / (\kappa R)} \sim \nu^2 N^2 R^3 \kappa / e^2. \quad (31)$$

The 2D linear screening radius produced by g_{min} is

$$r_s = \frac{\kappa}{2\pi g_{min} e^2} \sim \frac{1}{\nu^2 N^2 R^3}. \quad (32)$$

One can verify using Eq. (30) that $\gamma_{2D} \ll e^2 / \kappa R$ for such r_s and therefore long-range contribution can be neglected.

The growing part at $\nu < 1/2$ can be studied in the similar way as in 3D. That is, one can use the idea about 0-complex, 1-complex and 2-complex to find the Fermi level

$$\mu \sim -e^2 N^{1/2} / \kappa \quad (33)$$

and BDOGS at the Fermi level (at $\nu \ll 1$)

$$g_<(\mu) \sim \kappa \nu N^{1/2} / e^2. \quad (34)$$

For the maximum line of oscillating part, the collective typical fluctuation of potential energy is given by Eq. (30) and BDOGS at the Fermi level is

$$g_{max}(\mu) \sim \frac{N}{\gamma} \sim \frac{N^{1/2} \kappa}{e^2 \nu} \quad 1 \ll \nu < \nu_s = 1/\sqrt{NR^2}. \quad (35)$$

Here we dropped the logarithmic factor and therefore r_s disappeared from the equations. In this approximation unlike 3D situation, we do not need the self-consistent method. As a result $g_{max}(\mu)$ decreases with ν much slower than in 3D.

Both Eqs. (35) and (31) reach $g_s(\mu) \sim N/(e^2 / \kappa R)$ at $\nu \sim \nu_s = 1/\sqrt{NR^2}$, where the distinction between peaks and valleys disappears.

Up to now we discussed charging of two-dimensional array of dots by donors or a gate situated outside of dots. In some two-dimensional systems electrons may be provided to a dot by donors located close to the dots. This can be done, for example, by creating a two-dimensional gas with help of close layer of donors parallel to its plane and then by etching outside dots both the gas and the donor layer. If such dots are essentially two-dimensional and heavily doped, internally induced fluctuations can cause their charging, in contrary to what we said in introduction about three-dimensional dots. Indeed, in this case, fluctuations of number of electrons in the dot and correspondingly of the Fermi level decrease inverse proportionally to the dot radius. This decay is similar to the charging energy, so that ratio of these energies is just proportional to the ratio of kinetic and potential energies of electron in the dot²².

V. DENSE THREE-DIMENSIONAL ARRAYS OF DOTS

Until now we dealt with sparse arrays of dots where $NR^3 \ll 1$ as shown in Fig. 2 and 4. Let us discuss what happens when the small parameter NR^3 grows. The saturation filling factor $\nu_s = (NR^3)^{-1/4}$ decreases, which means the number of oscillations decreases as well. The

oscillations disappear at $\nu_s \sim 1$ when $NR^3 \sim 1$, i. e. when the typical separation between dots is of the order of the dot size.

Let us now concentrate on the other extreme (Fig. 5) where say cubic dots are closely packed in a cubic lattice with the period R and the width d of an insulator between dots is small ($d \ll R$). The insulator is uniformly doped by donors. We show below that at a large enough average number of donors per dot, $\nu > 1$, the BDOGS is smeared. On the other hand at $\nu \ll 1$ typical donors do not contribute to BDOGS at the Fermi level but rare clusters of donors result in a small BDOGS.

For the system of metallic cubic dots $\{i\}$ separated by a clean insulator, potentials ϕ_i and charges Q_i of dots are related by linear equations

$$\phi_i = \sum_j P_{ij} Q_j \quad (36)$$

and

$$Q_i = \sum_j C_{ij} \phi_j, \quad (37)$$

where P_{ij} is the reciprocal matrix of the capacitance matrix C_{ij} . The coefficients satisfy $P_{ij} = P_{ji}$, $0 \leq P_{ij} \leq P_{ii}$ and depend on the relative positions of i and j only. Without donors the Hamiltonian can be written as

$$H = \frac{1}{2} \sum_{ij} P_{ij} Q_i Q_j = \frac{1}{2} \sum_i P_{ii} Q_i^2 + \frac{1}{2} \sum_{i \neq j} P_{ij} Q_i Q_j. \quad (38)$$

Of course, it has minimum when all $Q_i = 0$.

In order to understand the role of ionized donors let us study an isolated donor between the dots A and B (Fig. 14). The positive donor is completely screened by negative charges q_A and q_B appearing on the surface of A and B, i. e. $q_A + q_B + e = 0$. These charges leave compensating positive charges $-q_A$ and $-q_B$ in the dots A and B. If x_A and x_B are distances from the donor to the dots A and B respectively then

$$q_A x_B = q_B x_A. \quad (39)$$

One can easily arrive at Eq. (39) imagining that the donor for a moment is replaced by the uniformly charged plane parallel to the faces of cube A and B (with the same x_A and x_B), and minimizing the sum of Coulomb energies of two emerging plane capacitors with distances between planes x_A and x_B as a function of q_A . Note that at $d \ll R$ all points of the charged plane are in the same conditions and the plane fields are just a superposition of fields of these charges. This means Eq. (39) should also hold for a point charge of this plane or just for a donor. Eq. (39) means that potentials of dot A and B are equal. In other words, the group made of the positive donor, q_A and q_B produces an electric field which is confined in

the vicinity of the donor. The group does not affect the electric potential of any dot. Therefore the group can be totally forgotten when we study the charges and potentials of the dots, or in other words it can be totally ignored in the Hamiltonian.

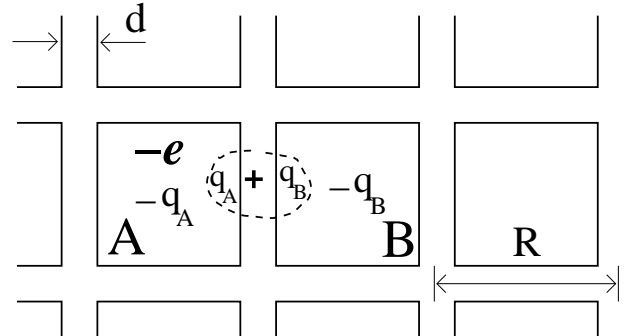


FIG. 14. Two-dimensional cross section through a donor (with charge $+e$) located between the dots A and B for the system shown in Fig. 5. The group within the dashed circle is neutral altogether and does not affect the energy levels of the dots A and B. The dot A gets an electron donated by the donor because the donor is closer to its border.

On the other hand, the compensating positive charges $-q_A$ and $-q_B$ can not be ignored. One can say that the donor's charge is split into two fractional parts $-q_A$ and $-q_B$. Charges $-q_i$ are uniformly distributed between 0 and e .

When there are more than one donor around a dot A we can simply add them up $Q_{AD} = -q_{A1} - q_{A2} - \dots$ to get the total positive charge induced by donors on the dot A.

Each donor also donates an electron to the array of dots. We assume that $d \gg a$, where a is the tunneling length of electrons in the insulator so that the conductance G between two dots is much smaller than e^2/h . In this case each dot can get only integer number of extra electrons n_i . The neutrality of the whole system requires $-e \sum n_i = \sum Q_{iD}$. For a given fractional set $\{Q_{iD}\}$ the integer set $\{n_i\}$ minimizes the Hamiltonian

$$H = \frac{1}{2} \sum_i P_{ii} (Q_{iD} - n_i e)^2 + \frac{1}{2} \sum_{i \neq j} P_{ij} (Q_{iD} - n_i e) (Q_{jD} - n_j e). \quad (40)$$

This energy is calculated from the reference point of the sum of energies of neutral groups around each donor, which does not depend on n_i . If each donated electrons were shared by dots this fractional charges would neutralize Q_{iD} and make $H = 0$ and all $\phi_i = 0$. This is equivalent to what would happen if all grain are grounded. Discreteness of n_i makes finding the ground state n_i non-trivial. It is clear that in the globally neutral system the chemical potential μ lies in the same place as for a system of neutral dots, i. e. $\mu = 0$. In the ground state we can introduce “one-dot” energies of an empty dot state above

the Fermi level assuming that charges of other dots are fixed

$$\varepsilon_i^{(e)} = H(n_i + 1) - H(n_i) = -e\phi_i + \frac{1}{2}P_{ii}e^2, \quad (41)$$

where

$$\phi_i = \sum_j P_{ij} (Q_j - n_j e) \quad (42)$$

is the electrostatic potential of the dot i . For an occupied state in the similar way

$$\varepsilon_i^{(o)} = H(n_i) - H(n_i - 1) = -e\phi_i - \frac{1}{2}P_{ii}e^2. \quad (43)$$

In the absence of donors when all dots are neutral, i. e. $\phi_i = 0$, we get $\varepsilon_i^{(e)} = +\frac{1}{2}P_{ii}e^2$ and $\varepsilon_i^{(o)} = -\frac{1}{2}P_{ii}e^2$. The single electron BDOGS for neutral dots looks the same as in Fig. 3 except the separation of peaks or the level spacing is smaller now $e^2P_{ii} \sim e^2/\kappa_{eff}R \simeq \frac{e^2d}{\kappa R^2}$ (the calculation of P_{ii} is in Appendix). Here

$$\kappa_{eff} \simeq \kappa R/d \quad (44)$$

is the effective dielectric constant of the array. For charged dots stability of the global ground state requires $\varepsilon_i^{(e)} > \mu = 0$ and $\varepsilon_i^{(o)} < \mu = 0$.

Let us study the BDOGS in the case when there are more than one donors per dot ($\nu \gg 1$). In order to find BDOGS we neglect the interaction terms in Eq. (40) and consider only diagonal terms. As a result the ground state of the system is realized by such a set of $\{n_i\}$ that $-e/2 \leq Q_{iD} - n_i e \leq e/2$. So effective charges on different dots in the ground state of the array are uniformly distributed from $-e/2$ to $e/2$. This gives the energy independent BDOGS

$$\tilde{g}_s(\varepsilon) \sim \frac{1}{e^2 P_{ii} R^3}. \quad (45)$$

Consider now the role of non-diagonal terms. At a big distance $r_{ij} \gg R$ the coefficients P_{ij} have the Coulomb form $P_{ij} \approx 1/\kappa_{eff}r_{ij}$. They, therefore, result in a density of ground states (DOGS) with the Coulomb gap at the Fermi level, which in turn leads to ES law.

The finite BDOGS at the Fermi level and ES law at $\nu \gg 1$, originates from random distribution of charges Q_i , which in turn is related to the fact that several donors contribute into each Q_{iD} . Even for nearest neighbor dots Q_{iD} and Q_{jD} are independent since they include contributions of different donors.

We turn now to the case of a small density of donors $\nu \ll 1$ and first deal with typical donors isolated from each other. As discussed above for such an isolated donor between the dots A and B, the charges induced by the donor are related by $Q_{AD} + Q_{BD} = +e$. If the donor is closer to the dot A, $Q_{AD} > e/2 > Q_{BD} > 0$. If we neglect interaction between the dots A and B in Eqs. (41)

and (43) we arrive at finite BDOGS of isolated donors at the Fermi level. States at the Fermi level are provided by dots where $Q_{BD} = 1/2 - \delta$ with $\delta \ll 1$. Then the dot B has a state just above the Fermi level and A has a state just below it. The fact that these states are so closely correlated in space leads to their elimination by the interaction between the dots A and B. Indeed, in the ground state the electron donated by the donor is on the dot A. The total charges on A and B is $Q_A = Q_{AD} - e = -Q_{BD}$ and $Q_B = Q_{BD}$. The electric potential on B is $\phi_B = P_{BB}Q_B + P_{BA}Q_A$ and according to Eq. (41) all the levels on B are moved down by $e\phi_B$. Using the fact $0 \leq Q_{BD} \leq e/2$, we have

$$0 \leq e\phi_B \leq (1 - \alpha)P_{BB}e^2/2, \quad (46)$$

where $\alpha \equiv P_{BA}/P_{AA} = 0.34 \pm 0.01$ represents the interaction between nearest neighbor dots (see the calculation of α in Appendix). According to Eq. (41) the lowest vacant level of dot B is at least $\alpha P_{ii}e^2/2$ above the Fermi level. Similarly, according to Eq. (43) the highest filled level on the dot A is moved up by $-e\phi_A$ with $0 \leq -e\phi_A \leq (1 - \alpha)P_{AA}e^2/2$ and it is at least $\alpha P_{ii}e^2/2$ below the Fermi level (Fig. 15).

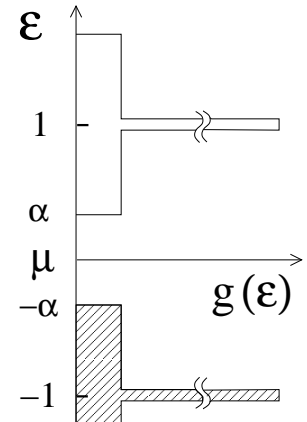


FIG. 15. BDOGS of isolated donors at $\nu \ll 1$. Energy ε is measured in units of $\alpha P_{ii}e^2/2$. There is a hard gap of the width $\alpha P_{ii}e^2$ around the Fermi level.

Thus, we showed that for $\nu \ll 1$ typical isolated donors have a substantial hard gap of width $\alpha P_{ii}e^2$ in their density of states. This gap can not be destroyed by long range interactions of such donors because they form neutral complexes and weakly interact with each other at long distances.

One can also think of a donor in the neutral complex with electron of the neighboring dot A as a hydrogen-like donor in a semiconductor. Then the hard gap obtained above is similar to Hubbard gap. The electric dipole made of a donor and an electron in principle can accept another electron with a weak binding energy, but the energy difference or Hubbard gap between the two electronic levels makes sure that only the lower level is filled in the ground state.

Up to now we talked about typical isolated donors at $\nu \ll 1$. In fact there are rare configurations that make a non-zero BDOGS at the Fermi level. Let us show how this happens.

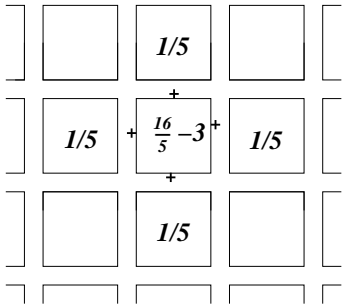


FIG. 16. An example of rare configurations leading to the finite BDOGS at the Fermi level at $\nu \ll 1$. The cluster of 5 dots and 4 donors is effectively positively charged in the ground state. Charges of 5 dots are shown in units of e . All the other dots in the vicinity of the cluster remain neutral.

Consider, for example, a cluster of 4 donors around one dot (Fig. 16). The charges of donors are shared by 5 dots in such a way that charge of each donor is effectively split into $4e/5$ going to the central dot and $e/5$ going to its nearest neighbor. The middle dot has effective charge $Q_{iD} = 16e/5$ and each of the four neighbor dots has $Q_{jD} = e/5$. Let us show that in the ground state of the cluster $n_i = 3$ for the central dot and $n_i = 0$ for all others, i. e. there are only three electrons on the cluster of four donors so that the cluster has a net charge $+e$. It is effectively shared by the 5 dots, each getting $+e/5$. According to Eq. (41) addition of the fourth electron to this cluster costs

$$\varepsilon_i^{(e)} = \left[-\frac{1}{5}(4\alpha + 1) + \frac{1}{2} \right] P_{ii} e^2 \approx 0.03 P_{ii} e^2 \quad (47)$$

where $\alpha = P_{12}/P_{11}$, and as shown in Appendix $\alpha = 0.3405$. This means that $\varepsilon_i^{(e)} > \mu = 0$ and the positively charged cluster of Fig. 16 is stable with respect of bringing the fourth neutralizing electron. The physical reason for such stability is uniform smearing of the net charge over 5 dots which diminishes potential of the cluster ϕ_i at the central dot attracting the fourth electron (the first term in the right side of Eq. (47)).

We have shown above an example of a positive “donor-like” cluster. Moving each of the four donors away from the central dot in the direction of the neighbor dot one can construct an “acceptor-like” cluster in which charge $-e$ is evenly shared by 5 dots. Such a cluster accepts an electron released by the cluster in Fig. 16. Thus, some clusters charge themselves by “self-compensation” similarly to amphoteric impurities in semiconductors. Of course, there are also neutral clusters and tuning positions of donors between dots one can continuously go from a neutral cluster to the charged one. This means

that BDOGS at the Fermi level created by clusters is finite.

Using coefficients P_{ij} calculated in Appendix, it is easy to find that the smallest charged cluster in the ground state is the cluster of 4 dots with 3 donors between them. Therefore, at $\nu \ll 1$ the BDOGS at the Fermi level grows as $g_0(\mu) \propto \nu^3$ and it begins to be significant at $\nu \sim 1$ (see Fig. 9).

The structure of self charging clusters discussed above is similar to the mechanism which provides a non-zero bare density of states in a system of quasi-one-dimensional electron crystals at low impurity concentration²³. There is also similarity to self-compensation of clusters of several donors in uncompensated semiconductor near the insulator-metal transition²⁴.

As we saw above in the “super-dense” array of dots with $d \ll R$, a large enough concentration of donors can easily smear BDOGS. This is a natural explanation of the experiments, where the ES law is observed. Let us consider parameter T_0 of the ES law (Eq. (1)) for a dense array of dots at $\nu \gg 1$. According to Ref.⁴ $T_0 \sim e^2/(\kappa_{eff}\xi)$, where ξ is the localization length for tunneling to distances much larger than R . When an electron tunnels through insulator it accumulates dimensionless action d/a , where a is the tunneling decay length in the insulator. On the distance x electron accumulates x/R such actions. Thus, its wave function decays as $\exp(-xd/Ra) = \exp(-x/\xi)$, where the localization length $\xi = aR/d$. This enhancement of localization length is similar to the one derived for disordered granular system near percolation threshold²⁵. It leads to

$$T_0 \sim \frac{e^2 d}{\kappa_{eff} a R} = \frac{e^2 d^2}{\kappa R^2 a} \quad (48)$$

We see that with decreasing d the temperature T_0 decreases as d^2 . This continues until conductance of the insulator layer $G = (e^2/\hbar)(Rk_F)^2 e^{-2d/a}$ reaches the quantum limit $G \sim e^2/\hbar$, i. e. while $d > d_c \equiv a \ln(Rk_F)$. At $d \ll d_c$ the characteristic ES temperature $T_0(d)$ should vanish when $d \rightarrow 0$, but the way how this happens is still unknown (see also recent publications^{26,27} concerned with the case $G \gg 1$).

In the above calculation of the localization length we assumed that tunneling through a metallic dot does not accumulate more action. Actually a dirty dot provides logarithmic contribution to the tunneling action²⁸. We assume that it is much smaller than $2d/a$ resulting from crossing the insulator.

Until now we discussed only the “super-dense” array shown in Fig. 5. Let us consider what happens in the system of almost densely packed metallic spheres (Fig. 17), where insulator occupies a larger fraction of space than in Fig. 5.

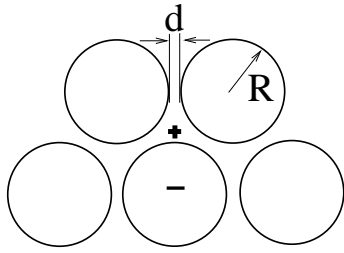


FIG. 17. An almost densely packed array of metallic spheres ($d \ll R$). A donor is shown by + and electron donated by it is shown by -.

One can show that in such a system BDOGS as a function of number of donors per dot ν behaves qualitatively similar to Fig. 9. At smaller ν only a cluster of donors around a dot can create a finite BDOGS, while at $\nu \gg 1$ donors easily smear BDOGS. In this case, characteristic temperature of ES law is $T_0 \approx e^2 d/aR$. It loses one power of d/R because the dielectric constant of such systems does not diverge at $d \rightarrow 0$. When distance between dots d grows and exceeds R , we get sparse periodic array (Fig. 13) and recover oscillations of BDOGS at $\nu \gg 1$. At $\nu \ll 1$ there is a smooth cross-over between two super-linear growths of BDOGS related to rare donor clusters in the vicinity of some dots.

Although we arrived at $\nu \gg 1$ as the universal criterion of substantial smearing of BDOGS for both dense arrays (Figs. 5 and 17) and sparse arrays (Figs. 2 and 13), we should understand that the required concentration of donors N_D in the insulator grows while volume fraction of insulator decreases from the arrays on Figs. 2 and 13 to the one on Fig. 17 and then to the one on Fig. 5.

In some cases metallic granules are first coated by the layer of a doped insulator (for example, the metal's oxide) and then compressed into the bulk array with a clean insulator of different kind of filling or just air filling empty space (Fig. 18). For simplicity we assume the dielectric constant of the coating insulator is close to that of the filling space between dots.

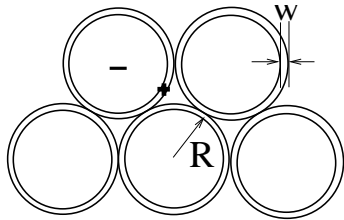


FIG. 18. An array of coated dots. The width of coating insulator is w . A donor is shown by + and electron donated by it is shown by -.

We would like to consider BDOGS for such a model of granular metal in order to understand cross-over between the studied above case of donors residing outside dots and those on the dot surface or inside dots. In the latter case, donors are screened and act as short range

neutral impurities. According to the introduction such impurities can not charge a neutral array of dots. Thus, effect of donors in the layer of the width $w \ll R$ should decrease as w vanishes.

Indeed, one can calculate, fluctuation of average the potential of donor layer of the width w which plays the role of fluctuation of work function of dots. It can be estimated as a potential created by the layer of the width w by fluctuating concentration $(N_D w R^2)^{1/2}/w R^2$. One can imagine that, correction to the work function is created by effective random double layer. Such correction to the work function is of order $e^2((N_D w^3)^{1/2}/\kappa R$. It becomes larger than the charging energy only at $N_D w^3 \gg 1^{29}$. This condition of BDOGS smearing is obviously much stronger than “one donor per dot” condition valid for a uniform insulator. When w approaches the lattice constant the role of donors is so much weakened that in order to smear BDOGS one needs the relative concentration of donors to be of the order of 50%. At the surface, donors and their images are still forming dipoles with fluctuating dipole moments, which create fluctuating double layer potential. On the other hand, when donors enter inside the dot, each donor becomes exponentially screened from all sides, the dipoles and the random double layer disappear. This diminishes the role of donors further so that as we said in introduction even large concentration of impurities inside the whole three dimensional dot can not charge the dot.

VI. CONCLUSION

This paper addresses the problem of explanation of the temperature dependence of the conductivity observed in granular metals and arrays of quantum dots. We show that ES law is the most natural explanation for this dependence (in spite of recently expressed doubts³⁰). For this purpose we present a simple model with random charging of clean metallic dots in both sparse and dense arrays of dots. In both cases we assume that the insulator separating dots is uniformly doped by donors, which donate their electrons to dots. Random positions of dots in the sparse case (Fig. 1) and random positions of donors in the dense periodic model (Fig. 5) lead to random charging of dots in the global ground state and to filling of the gap of the bare density of individual dots at the Fermi level. The long range Coulomb interaction creates a soft Coulomb gap on the background of the finite bare density of ground states in the vicinity of the Fermi level. At low enough temperature this leads to the ES variable range hopping conductivity, in agreement with multiple experimental observations.

We concentrate on the dependence of the bare density of states on a number of donors per dot. Such dependence for the sparse and dense models are shown in Fig. (7) and Fig. (9) are qualitatively different. The sparse random model shows linear growth of BDOGS at weak

doping and oscillations of the density of states at strong doping. On the other hand the dense model shows very small density of states at weak doping and no oscillations at stronger doping. The bare density of states determines the width of the Coulomb gap and the characteristic temperature of transition from ES law to Mott's law with increasing temperature. It determines many thermodynamic properties of the array as well.

For dense arrays we have calculated characteristic temperature T_0 of ES law in the case, when tunneling conductance between granules is small. The challenging question of calculation of T_0 in the case of even closer dots will be addressed in the next publication. Another interesting question left beyond the scope of this paper is the origin of ES law in isotropic and anisotropic arrays of strongly anisotropic (elongated) granules, for example, nano-tubes.

In this paper we concentrated on ohmic hopping conductivity. However, our results can be applied to non-ohmic conductivity, too. It was shown³¹ that at low temperatures a strong electric field E replaces temperature T in the exponential temperature dependence of the variable range hopping by the effective temperature $T_E = eE\xi/2k_B$. As a result non-ohmic ES law reads $j = j_0 \exp[-(E_0/E)^{1/2}]$ with $E_0 = 2T_0/e\xi$. This dependence was observed in granular metals and nanocrystal thin films^{1,11}.

ACKNOWLEDGMENTS

We are grateful to M. V. Entin, M. M. Fogler, Yu. M. Galperin, A. Kamenev and A. I. Larkin for helpful discussions. This work was partially supported by NSF No. DMR-9985785.

APPENDIX: MATRIX ELEMENTS P_{ij} FOR NEIGHBORING DOTS.

Here we study the coefficients P_{ij} in Eq. (36). We know the diagonal term $P_{ii} \sim 1/\kappa_{eff}R$, and for distant neighbors $r_{ij} \gg R$ one can show that $P_{ij} \sim 1/\kappa_{eff}r_{ij}$. But the coefficients between close neighbors require further consideration.

The dense array of periodic dots is equivalent to the lattice of identical capacitors connecting adjacent dots. Such a system can be studied in the language of an equivalent resistor network. Imagine a cubic lattice network with an identical resistance between every nearest neighbor sites. Suppose that current I goes into a lattice site A and travels out through the network to infinity. Label the potential of site A to be V , the potential of nearby dots B, C, D, \dots to be $\alpha_{AB}V, \alpha_{AC}V, \alpha_{AD}V, \dots$. What are the values of the $\alpha_{AB}, \alpha_{AC}, \alpha_{AD}$, and so on? Here we are using the dimensionless coefficients such as

$\alpha_{AB} \equiv P_{AB}/P_{AA}$, and we know all of them are between 0 and 1.

A standard numerical calculation uses the fact that the current going into a site equals the current going out of it (Kirchhoff law), which means the potential of a site equals the average potential of its nearest neighbors. Using lattices of $N \times N \times N$ sites and keeping the potential at central site to be 1 and that of boundaries to be 0, one adjusts the potential values of the other sites so that the potential of each site is very close to the average potential of its nearest neighbors. Using lattices with N up to 97 we find $\alpha \equiv \alpha_{01} = 0.34 \pm 0.005$, $\alpha_{02} = 0.166 \pm 0.005$, $\alpha_{03} = 0.106 \pm 0.005$, $\alpha_{11} = 0.216 \pm 0.005$, $\alpha_{111} = 0.17 \pm 0.005$ (here 111 represents the vector between the two dots measured in the units of the lattice constant).

There is also an analytic way to find the coefficients³². Imagine the situation when there is charge Q_0 on the central dot while all the other dots remain neutral, one can use the equation similar to Kirchhoff law mentioned above

$$\phi(\vec{r}) - \frac{1}{6} \sum_{\vec{r}'} \phi(\vec{r}') = \frac{Q_0 d}{6\kappa R^2} \delta_{\vec{0}, \vec{r}} , \quad (49)$$

where \vec{r}' are 6 nearest neighbor of the site \vec{r} , and $\phi(\vec{r})$ is defined only on the discrete sites $\vec{r} = (n_x R, n_y R, n_z R)$. Eq. (49) can be solved using discrete Fourier transform

$$\phi_{\vec{k}} - \frac{1}{6} \phi_{\vec{k}} \cdot (\cos k_x R + \cos k_y R + \cos k_z R) = \frac{Q_0 d}{6\kappa R^2} . \quad (50)$$

One can find $\phi_{\vec{k}}$ and

$$\phi(\vec{r}) = \frac{dQ_0}{2\kappa R^2} \int_{BZ} \frac{d^3 k}{(2\pi)^3} \frac{R^3 \cos(\vec{k} \cdot \vec{r})}{3 - \cos k_x R - \cos k_y R - \cos k_z R} \quad (51)$$

where the integration is over the Brillouin zone $k_x, k_y, k_z \in (-\pi/R, \pi/R)$. One can use numerical integration to find

$$P_{00} \equiv \frac{\phi(\vec{0})}{Q_0} = \frac{0.2527d}{\kappa R^2}, \quad \alpha \equiv \alpha_{01} = \frac{P_{01}}{P_{00}} = 0.3405, \\ \alpha_{02} = 0.1697, \quad \alpha_{03} = 0.1089, \quad \alpha_{11} = 0.2183 \quad (52)$$

and so on. These results agree with the results of the first method.

¹ P. Sheng, B. Abeles, and Y. Arie, Phys. Rev. Lett. **31**, 44 (1973); B. Abeles, P. Sheng, M. D. Coutts, and Y. Arie, Adv. Phys. **24**, 407 (1975).

² S. Barzilai, Y. Goldstein, I. Balberg, and J. S. Helman, Phys. Rev. B **23**, 1809 (1981); N. Savvides, S. P. McAlister, and C. M. Hurd, Can. J. Phys. **60**, 1484 (1982); R. W. Simon, B. J. Dalrymple, D. Van Vechten, W. W. Fuller, and S. A. Wolf, Phys. Rev. B **36**, 1962 (1987); A. Gerber, A. Milner, G. Deutscher, M. Karpovsky, and A. Gladkikh, Phys. Rev. Lett. **78**, 4277 (1997).

³ L. Murawski, B. Koscielska, R. J. Barczynski, M. Gazda, and B. Jusz, Philos. Mag. B **80**, 1093 (2000).

⁴ B. I. Shklovskii and A. L. Efros, *Electronic Properties of Doped Semiconductors*, Springer-Verlag, New-York, 1984.

⁵ T. Chui, G. Deutscher, P. Lindenfeld, and W. L. McLean, Phys. Rev. B **23**, 6172 (1981).

⁶ M. Pollak and C. J. Adkins, Philos. Mag. B **65**, 855 (1992).

⁷ S. T. Chui, Phys. Rev. B **43**, 14274 (1991).

⁸ E. Cuevas, M. Ortuno, and J. Ruiz, Phys. Rev. Lett. **71**, 1871 (1993).

⁹ E. M. Baskin and M. V. Entin, Pis. Zh. Eksp. Theor. Fiz. **70**, 510 (1999) [JETP Lett. **70**, 520 (1999)].

¹⁰ A. I. Yakimov, A. V. Dvurechenskii, V. V. Kirienko, Yu. I. Yakovlev, A.I. Nikiforov, and C. J. Adkins, Phys. Rev. B **61**, 10868 (2000); A. I. Yakimov, A. V. Dvurechenskii, A. I. Nikiforov, and A. A. Bloshkin, Pis. Zh. Eksp. Theor. Fiz. **77**, 445 (2003) [JETP Lett. **77**, 376 (2003)].

¹¹ D. Yu, C. Wang, B. L. Wehrenberg and P. G. Guyot-Sionnest, cond-mat/0403597.

¹² A. L. Efros and B. I. Shklovskii, J. Phys. C **8**, L49 (1975).

¹³ A. Miller and E. Abrahams, Phys. Rev. **120**, 745 (1960).

¹⁴ Baskin and Entin⁹ postulated that excited states bring some dots into infinite percolation cluster of resistances and lead to exponentially larger hopping conductivity than ground states. In this way they obtained a new exponential factor of hopping conductivity where power 2/5 replaces power 1/2 in ES law. We disagree with this claim because filling of a dot by electrons is controlled by the ground state.

¹⁵ Ref.⁴, Chapter 3; A. L. Efros, B. I. Shklovskii, I. Y. Yanchev, Phys. Stat. Sol. B **50**, 45 (1972).

¹⁶ S. D. Baranovskii, B. I. Shklovskii, and A. L. Efros, Zh. Eksp. Teor. Fiz. **87**, 1793 (1984) [Sov. Phys. JETP **60** 1031 (1984)].

¹⁷ A. L. Efros and B. I. Shklovskii, in *Electron-Electron interaction in disordered systems*, ed. by A. L. Efros and M. Pollak. North-Holland, Amsterdam 1985.

¹⁸ D. Yu, C. Wang, and G. P. Guyot-Sionnest, Science, **300**, 1227 (2003).

¹⁹ G. Medeiros-Ribeiro, F. G. Pikus, P. M. Petroff, A. L. Efros, Phys. Rev. B **55**, 1568 (1997).

²⁰ T. P. Smith III, W. I. Wang, and P. J. Stiles, Phys. Rev. **34**, 2995 (1986).

²¹ F. Stern, Phys. Rev. B **9**, 4597 (1974).

²² We are grateful to M. Entin for attracting our attention to this situation.

²³ M. M. Fogler, S. Teber and B. I. Shklovskii, Phys. Rev. B **69**, 035413 (2004).

²⁴ R. N. Bhatt, T. M. Rice, Phys. Rev. B **23**, 1920 (1981).

²⁵ B. I. Shklovskii, Fiz. Tsv. Tela, **26**, 585 (1984) [Sov. Phys. Solid State **26**(2), 353 (1984)].

²⁶ V. Tripathi, M. Turlakov, cond-mat/0307534.

²⁷ J. S. Meyer, A. Kamenev, and L. I. Glazman, cond-mat/0401343.

²⁸ D. V. Averin and Yu. V. Nazarov, Phys. Rev. Lett. **65**, 2446 (1990).

²⁹ Alternatively, one can derive the same inequality using idea of fractionalization of a donor charge. In the case of coated dots, the host dot of the donor gets all but a fraction of the order of w/R of its charge, which is acquired by the host dot nearest neighbors. The non-integer part of the host dot charge reaches $e/2$ only when fluctuation of number of donors in the coating layer $(N_D R^2 w)^{1/2}$ multiplied by w/R becomes of the order of unity. This brings us back to $N_D w^3 \gg 1$.

³⁰ K. B. Efetov and A. Tschersich, Phys. Rev. B **67**, 174205 (2003).

³¹ B. I. Shklovskii, Fiz. Tekh. Poluprov. 6, 2335 (1973) [Sov. Phys.-Semicond. **6**, 1964 (1973)].

³² This solution was suggested to us by M. M. Fogler.